Aerial Intelligent Reflecting Surface for Secure MISO Communication Systems

Zhen Liu[1], Zhengyu Zhu[1,2(✉)], Wanming Hao[1,2], and Jiankang Zhang[2]

[1] Henan Institute of Advanced Technology, Zhengzhou University, Zhengzhou, China
ieliuzhen@gs.zzu.edu.cn, zhuzhengyu6@gmail.com, iewmhao@zzu.edu.cn
[2] School of Information Engineering, Zhengzhou University, Zhengzhou, China
iejkzhang@zzu.edu.cn

Abstract. In this paper, an aerial intelligent reflecting surface (AIRS) is introduced to assist the ground secure communication system, where intelligent reflecting surface shifts the communication channel to target position and AIRS can be flexibly deployed in the air. We aim to maximize the secure communication rate of the system, and the formulated problem is difficult to solve. To this end, the problem is decomposed into three sub-problems, and an efficient iterative algorithm is proposed by jointly optimizing the transmission beamforming, the reflection phase shift and trajectory of the AIRS with the alternating optimization technique. The semi-definite relaxation is used to optimize the AIRS's phase shift, and the successive convex approximation method is applied to solve the non-convex trajectory optimization sub-problem. Numerical results show that the secrecy rate of the proposed algorithm precedes the benchmark schemes, and the AIRS has found the same optimal position with respect to different origins.

Keywords: Aerial intelligent reflecting surface · Secure communication · MISO system · Alternating optimization

1 Introduction

Nowadays, sixth-generation (6G) network are developing rapidly to meet the large-scale communication needs, especially in flexible, high-speed, secure communication, etc. Intelligent reflecting surface (IRS), as a new wireless device, can smartly reflect the signal through exhaustive low-cost passive reflecting elements and is always used to alter the transmission of radio signals over the wireless network [1].

This work was supported in part by the National Natural Science Foundation of China under Grant 61801434, 61571401, 61801435, and 61771431, in part by the Project funded by China Postdoctoral Science Foundation under Grant 2020M682345, in part by the Henan Postdoctoral Foundation under Grant 202001015, in part by the Innovative Talent of Colleges and University of Henan Province under Grant 18HASTIT021, in part by the Science and Technology Innovation Project of Zhengzhou under Grant 2019CXZX0037.

H. Gao et al. (Eds.): ChinaCom 2021, LNICST 433, pp. 553–566, 2022.
https://doi.org/10.1007/978-3-030-99200-2_41

IRS shows great potential to enhance physical layer security. Wei Sun studied the security issue of the IRS aided simultaneous wireless information and power transfer system, in which the transmit beamforming and artificial noise at the base station (BS) and the reflective beamforming at the IRS are jointly designed to maximize the secrecy rate to the receivers [2]. The transmit beamforming and the reflective beamforming of the IRS are jointly designed to maximize the secrecy rate of multiple input single output (MISO) communication system [3]. The author in [4] further complete the outage constrained robust design for IRS system, which takes the artificial noise into consideration.

On the other hand, unmanned aerial vehicle (UAV) can act as a mobile relay or air BS to aid the secure communication in different scenarios [5,6]. Furthermore, UAV is able to build the line-of-sight (LOS) dominant transmission links with the ground users, and IRS can smartly adjust their reflecting elements for passive phase shift. It is proposed that UAV carrying an IRS serves as a mobile relay to assist the ground communication [7–9]. New methods have been discussed in [10] by jointly applying IRS and UAV in integrated air-ground wireless networks.

Motivated by the benefits of the IRS and the mobile UAV, we consider an aerial intelligent reflecting surface (AIRS), which can be flexibly deployed and adjust the phase shift simultaneously. The transmit beamforming, the phase shift and trajectory of the AIRS are jointly optimized to assist secure MISO communication system. Our goal is to maximize the secrecy rate, and the main contributions are summarized as follows:

- The maximization of secrecy rate problem is difficult to solve due to the non-convexity of the objective function and multiple coupled variables. An alternating optimization (AO) method is applied to solve the three sub-problems, where the variables are optimized in an iterative manner.
- For the transmit beamforming vector, we obtain a closed-form solution in sub-problem 1, and the reflection phase shift of AIRS is solved by the semi-definite relaxation (SDR) method in sub-problem 2. In sub-problem 3 of the AIRS's optimal positon, we first introduce auxiliary variables to simplify the objective function and decouple the position variable. Then we apply the successive convex approximation (SCA) method to reformulate the non-convex trajectory problem into an approximated convex problem.
- Simulation results are provided to verify the effectiveness and convergence of the proposed AO algorithm, which precedes the benchmark schemes without phase shift optimization and fixed AIRS. Besides, the AIRS has found the same optimization position in different origins situation.

2 System Model and Problem Formulation

2.1 System Model

In this paper, we consider an AIRS-based MISO communication system, in which the UAV is equipped with an IRS as a passive relay, and an eavesdropper attempts to wiretap the legitimate communication between the BS and the user

on the ground. The AIRS is equipped with $N = N_x \times N_y$ reflecting elements, whose phase can be manipulated by the controller on the UAV, and N_x, N_y are passive reflection units which are spanned as a uniform planar array. We assume the BS is equipped with M antennas arranging in alignment, and the user and eavesdropper are equipped with a single antenna, respectively.

Without loss of generality, all nodes are placed in the three-dimensional (3D) Cartesian coordinate system. The BS, user, and eavesdropper are fixed on the ground, whose horizontal coordinates can be denoted by $\mathbf{C}_B = [x_B, y_B]$, $\mathbf{C}_U = [x_U, y_U]$ and $\mathbf{C}_E = [x_E, y_E]$, respectively. The coordinate of AIRS is denoted by $\mathbf{C}_I = [x_I, y_I, z_I]$, and it can travel at a constant altitude z_I. In addition, the AIRS is constrained by flying within a certain horizontal range as

$$\mathbf{C}_I \in \mathcal{X} \times \mathcal{Y}. \tag{1}$$

where $\mathcal{X}$ and $\mathcal{Y}$ denoted the feasible region of the UAV deployment in the x-asix and y-axis, respectively [9].

We assume that the nodes communicate with the AIRS are denoted by the set of $Z \in \{B, U, E\}$, the elements of Z represent the BS, the user, and the eavesdropper, respectively. The reflection elements of AIRS are arranged in a rectangular matrix, and then the channel coefficient of the antenna of Z with the AIRS can be expressed as

$$\mathbf{v}_{ZI} = \mathbf{v}_x \otimes \mathbf{v}_y, \tag{2}$$

where $\mathbf{v}_x$ and $\mathbf{v}_y$ are set as $\mathbf{v}_x = [1, e^{-j\frac{2\pi\Delta d}{\lambda}\varphi_{ZI}}, ..., e^{-j\frac{2\pi\Delta d}{\lambda}(N_x-1)\varphi_{ZI}}]^T$ and $\mathbf{v}_y = [1, e^{-j\frac{2\pi\Delta d}{\lambda}\phi_{ZI}}, ..., e^{-j\frac{2\pi\Delta d}{\lambda}(N_y-1)\phi_{ZI}}]^T$, and they denote the channel coefficient of the link from one antenna to the elements of N_x and N_y in the AIRS, respectively. Here, φ_{ZI} and ϕ_{ZI} represent the azimuth and elevation angles of the AIRS component, which can be denoted as $\varphi_{ZI} = \frac{x_I - x_Z}{d_{ZI}}$ and $\phi_{ZI} = \frac{z_I - z_Z}{d_{ZI}}$. In the above formulas, d_{ZI} represents the distance between the antenna of Z and the AIRS. Constants Δd and λ denote the reflecting element separation at the AIRS and the carrier wavelength, respectively. x_Z and z_Z represent the coordinates of the x-axis and z-axis of Z, respectively. Since AIRS constantly moves throughout the process, $\mathbf{v}_{ZI}$ changes with the coordinate of AIRS [11].

In this situation, the channels related to the AIRS are dominated by LOS component. By applying the existing channel estimation techniques, we assume the channel state information (CSI) of AIRS-related channels can be obtained based on the method in [12]. Accordingly, the channel gains between the AIRS with the user and eavesdropper can be expressed as

$$\mathbf{h}_{UI} = \sqrt{\rho d_{UI}^{-\alpha}} * \mathbf{v}_{UI}, \tag{3a}$$

$$\mathbf{h}_{EI} = \sqrt{\rho d_{EI}^{-\alpha}} * \mathbf{v}_{EI}, \tag{3b}$$

where ρ is the pass loss coefficient of the reference distance $D_0 = 1$m. d_{UI} denotes the distance between the AIRS and the user, and d_{EI} is the same as

d_{UI}. Constant α represents the corresponding path loss exponent related to the ground-air (G-A) link. $\mathbf{v}_{UI}$ and $\mathbf{v}_{EI}$ represent the channel coefficient of the AIRS with the user and eavesdropper, which are in the form of $\mathbf{v}_{ZI}$ with $Z \in \{B, U, E\}$.

The M antennas of the BS arrange in linear planar. Since the antenna separation is weeny compared to the distance between the BS and the AIRS, the channel coefficients of diffierent antennas of BS with the AIRS are treated as the same. Then, the channel gain between the BS and the AIRS can be expressed as

$$\mathbf{H}_{BI} = \sqrt{\rho d_{BI}^{-\alpha}}\mathbf{v}_{BI} * [1, e^{-j\frac{2\pi \Delta a}{\lambda}}\phi_{BI}, ..., e^{-j\frac{2\pi \Delta a}{\lambda}(M-1)}\phi_{BI}] = \sqrt{\rho d_{BI}^{-\alpha}}\mathbf{V}_{BI}, \quad (4)$$

where d_{BI} denotes the distance between the BS and the AIRS. $\mathbf{v}_{BI}$ is the channel coefficient between the BS and the AIRS. Δa represents the antenna separation at the BS. ϕ_{BI} is the elevation angles of the BS with the AIRS, and $\mathbf{V}_{BI} = \mathbf{v}_{BI} * [1, e^{-j\frac{2\pi \Delta a}{\lambda}}\phi_{BI}, ..., e^{-j\frac{2\pi \Delta a}{\lambda}(M-1)}\phi_{BI}]$.

We assume that the channels of the gorund-ground (G-G) communication link follow Rayleigh fading, and then the channel gains of the BS-user link and the BS-eavesdropper link can be expressed as

$$\mathbf{h}_{BU} = \sqrt{\rho d_{BU}^{-\kappa}} * \mathbf{g}_{BU}, \quad (5a)$$

$$\mathbf{h}_{BE} = \sqrt{\rho d_{BE}^{-\kappa}} * \mathbf{g}_{BE}, \quad (5b)$$

where d_{BU} and d_{BE} are the distance from the BS to the user and eavesdropper, κ is the corresponding path loss exponent related to the G-G link. $\mathbf{g}_{BU}$ and $\mathbf{g}_{BE}$ denote the small-scale fading, which represent the random scattering component modeled by a circularly symmetric complex Gaussian (CSCG) distribution featuring zero-mean and unit-variance. Therefore, we can obtain $\mathbf{H}_{BI} \in \mathbb{C}^{N\times M}$, $\mathbf{h}_{EI} \in \mathbb{C}^{N\times 1}$, $\mathbf{h}_{UI} \in \mathbb{C}^{N\times 1}$, $\mathbf{h}_{BU} \in \mathbb{C}^{1\times M}$, $\mathbf{h}_{BE} \in \mathbb{C}^{1\times M}$, respectively.

The BS transmits a confidential message to the user via beamforming $\mathbf{w} \in \mathbb{C}^{M\times 1}$, which satisfies the following constraint

$$||\mathbf{w}||^2 \leqslant P_{BS}, \quad (6)$$

where P_{BS} denotes the BS's maximum transmit power. Moreover, the signals from BS are reflected by AIRS in adjustable phase shift, and the reflection phase of the AIRS is modeled by using $\mathbf{q} \triangleq [q_1, ..., q_N]^T$, where $q_n = \beta_n e^{j\theta_n}$, $\beta_n \in [0, 1]$ and $\theta_n \in [0, 2\pi)$ denote the amplitude reflection coefficient and phase shift of the n-th element, respectively. For simplicity, $\beta_n = 1, \forall n$ is set to achieve the maximum reflecting power gain, thus the elements of $\mathbf{q}$ should satisfy

$$||q_n|| = 1, \forall n. \quad (7)$$

Due to the severe path loss, ignoring the signal reflected twice or more by the AIRS, the signal received by the user and the eavesdropper can be respectively expressed as

$$y_U = (\mathbf{h}_{UI}^T \mathbf{Q}\mathbf{H}_{BI} + \mathbf{h}_{BU})\mathbf{w} + n_U, \quad (8)$$

$$y_E = (\mathbf{h}_{EI}^T \mathbf{Q} \mathbf{H}_{BI} + \mathbf{h}_{BE})\mathbf{w} + n_E, \tag{9}$$

where $\mathbf{Q}$ denotes the diagonal matrix of the vector $\mathbf{q}$. n_U and n_E denote the additive white Gaussian noises with mean zero and unit variances.

2.2 Problem Formulation

Based on (8) and (9), the signal noise ratio (SNR) of the user and eavesdropper are expressed as

$$\gamma_U = \frac{|(\mathbf{h}_{UI}^T \mathbf{Q} \mathbf{H}_{BI} + \mathbf{h}_{BU})\mathbf{w}|^2}{\sigma_U^2}, \tag{10a}$$

$$\gamma_E = \frac{|(\mathbf{h}_{EI}^T \mathbf{Q} \mathbf{H}_{BI} + \mathbf{h}_{BE})\mathbf{w}|^2}{\sigma_E^2}, \tag{10b}$$

where σ_U^2 and σ_E^2 denote the noise power at the user and eavesdropper, respectively. Therefore, the communication rates of the user and eavesdropper are obtained by using the Shannon formula, which are respectively expressed as

$$R_U = \log_2(1 + \gamma_U), \tag{11a}$$

$$R_E = \log_2(1 + \gamma_E), \tag{11b}$$

and the secrecy rate is expressed as $R_{\text{sec}} = R_U - R_E$.

We aim to get the maximum communication security rate by jointly optimizing the AIRS's trajectory, the phase shift matrices, and the BS's active beamforming. Therefore, the considered problem is formulated as follows

$$\text{P0:} \max_{\mathbf{w},\mathbf{Q},\mathbf{C}_I} \quad R_{sec} = R_U - R_E, \tag{12a}$$

$$\text{s.t. } \mathbf{C}_I \in \mathcal{X} \times \mathcal{Y}, \tag{12b}$$

$$\|\mathbf{w}\|^2 \leqslant P_{\text{BS}}, \tag{12c}$$

$$\|q_n\| = 1, \forall n. \tag{12d}$$

Since the objective function R_{sec} is non-convex with respect to the variables $\mathbf{w}, \mathbf{Q}$ and $\mathbf{C}_I$, it is difficult to directly obtain the optimal solution to the P0, and the constraints (12b)–(12d) are independent of these variables. In the next section, we propose an efficient algorithm to solve the P0 approximately.

3 Proposed Algorithm

In P0, the constraints of (12c) and (12d) are associated with only one variable $\mathbf{w}$ and $\mathbf{Q}$, respectively. Besides, the CSI of the communication channels $\mathbf{H}_{BI}$, $\mathbf{h}_{IU}$, $\mathbf{h}_{IE}$ are all related to the position of AIRS, which constrained by the traveling range of AIRS (12b). This motivates us to divide the P0 into three sub-problems about $\mathbf{w}, \mathbf{Q}$ and $\mathbf{C}_I$, respectively, and we propose an algorithm based on the AO method [14] to solve these sub-problems.

3.1 Sub-problem 1: Optimizing the Transmit Beamforming w with Given Q and $\mathbf{C}_I$

According to (10), the SNR of the user and the eavesdropper can be transformed respectively as follows

$$\begin{aligned}\gamma_U &= \frac{|(\mathbf{h}_{UI}^T\mathbf{Q}\mathbf{H}_{BI}+\mathbf{h}_{BU})\mathbf{w}|^2}{\sigma_U^2} \\ &= \mathbf{w}^H\frac{(\mathbf{h}_{UI}^T\mathbf{Q}\mathbf{H}_{BI}+\mathbf{h}_{BU})^H(\mathbf{h}_{UI}^T\mathbf{Q}\mathbf{H}_{BI}+\mathbf{h}_{BU})}{\sigma_U^2}\mathbf{w} \\ &= \mathbf{w}^H\eta_U\mathbf{w},\end{aligned} \tag{13a}$$

$$\begin{aligned}\gamma_E &= \frac{|(\mathbf{h}_{EI}^T\mathbf{Q}\mathbf{H}_{BI}+\mathbf{h}_{BE})\mathbf{w}|^2}{\sigma_E^2} \\ &= \mathbf{w}^H\frac{(\mathbf{h}_{EI}^T\mathbf{Q}\mathbf{H}_{BI}+\mathbf{h}_{BE})^H(\mathbf{h}_{EI}^T\mathbf{Q}\mathbf{H}_{BI}+\mathbf{h}_{BE})}{\sigma_E^2}\mathbf{w} \\ &= \mathbf{w}^H\eta_E\mathbf{w},\end{aligned} \tag{13b}$$

where $\eta_U \triangleq \frac{(\mathbf{h}_{UI}^T\mathbf{Q}\mathbf{H}_{BI}+\mathbf{h}_{BU})^H(\mathbf{h}_{UI}^T\mathbf{Q}\mathbf{H}_{BI}+\mathbf{h}_{BU})}{\sigma_U^2}$, $\eta_E \triangleq \frac{(\mathbf{h}_{EI}^T\mathbf{Q}\mathbf{H}_{BI}+\mathbf{h}_{BE})^H(\mathbf{h}_{EI}^T\mathbf{Q}\mathbf{H}_{BI}+\mathbf{h}_{BE})}{\sigma_E^2}$. For the given AIRS's position $\mathbf{C}_I$ and phase shift $\mathbf{Q}$, we can obtain the CSI in (13), hence the η_U and η_E are all constants. Then, the sub-problem 1 can be expressed as

$$\text{P1:}\max_{\mathbf{w}} \ \frac{\mathbf{w}^H\eta_{\mathrm{U}}\mathbf{w}+1}{\mathbf{w}^H\eta_{\mathrm{E}}\mathbf{w}+1}, \tag{14a}$$

$$\text{s.t. } \mathbf{w}^H\mathbf{w} \leqslant P_{\mathrm{BS}}. \tag{14b}$$

According to [3], the closed-form solution of P1 can be achieved as

$$\mathbf{w}_{opt} = \sqrt{P_{\mathrm{BS}}}\mathbf{v}_{\max}, \tag{15}$$

where $\mathbf{v}_{\max}$ is the normalized eigenvector corresponding to the largest eigenvalue of the matrix $(\eta_E + \frac{1}{P_{BS}}\mathbf{I}_M)^{-1}(\eta_U + \frac{1}{P_{BS}}\mathbf{I}_M)$, and $\mathbf{I}_M$ denotes an M-dimension identity matrix.

3.2 Sub-problem 2: Optimizing the AIRS Reflect Phase Shift Matrix Q with Given w and $\mathbf{C}_I$

With the optimal beamforming $\mathbf{w}^*$ obtained by solving P1, and the given AIRS's position $\mathbf{C}_I$, we can simplify the original problem P0 as the following optimization problem only about the refleciton phase shift $\mathbf{Q}$ of AIRS, which can be formulated as

$$\text{P2:} \max_{\mathbf{Q}} \ \frac{\frac{1}{\sigma_U^2}|(\mathbf{h}_{UI}^T\mathbf{Q}\mathbf{H}_{BI}+\mathbf{h}_{BU})\mathbf{w}|^2+1}{\frac{1}{\sigma_E^2}|(\mathbf{h}_{EI}^T\mathbf{Q}\mathbf{H}_{BI}+\mathbf{h}_{BE})\mathbf{w}|^2+1}, \tag{16a}$$

$$\text{s.t.} \ \ \|q_n\|=1, \forall n. \tag{16b}$$

By applying $\mathbf{h}_{UI}^T\mathbf{Q}\mathbf{H}_{BI}=\mathbf{q}^T diag(\mathbf{h}_{UI})\mathbf{H}_{BI}$ and $\mathbf{h}_{EI}^T\mathbf{Q}\mathbf{H}_{BI}=\mathbf{q}^T diag(\mathbf{h}_{EI})\mathbf{H}_{BI}$, we can further respectively transform the numerator and denominator of (16a) into the following equations by setting $\mathbf{s}=[\mathbf{q}^T,1]$,

$$\frac{1}{\sigma_U^2}|(\mathbf{h}_{UI}^T\mathbf{Q}\mathbf{H}_{BI}+\mathbf{h}_{BU})\mathbf{w}|^2=\mathbf{s}\mathbf{G}_U\mathbf{s}^H+h_U, \tag{17a}$$

$$\frac{1}{\sigma_E^2}|(\mathbf{h}_{EI}^T\mathbf{Q}\mathbf{H}_{BI}+\mathbf{h}_{BE})\mathbf{w}|^2=\mathbf{s}\mathbf{G}_E\mathbf{s}^H+h_E, \tag{17b}$$

where $h_U=\frac{\mathbf{h}_{BU}^*\mathbf{w}^*\mathbf{w}^T\mathbf{h}_{BU}^T}{\sigma_U^2}$, $h_E=\frac{\mathbf{h}_{BE}^*\mathbf{w}^*\mathbf{w}^T\mathbf{h}_{BE}^T}{\sigma_E^2}$, and

$$\mathbf{G}_U=\frac{1}{\sigma_U^2}\begin{bmatrix} diag(\mathbf{h}_{UI}^*)\mathbf{H}_{BI}^*\mathbf{w}^*\mathbf{w}^T\mathbf{H}_{BI}^T diag(\mathbf{h}_{UI}) & diag(\mathbf{h}_{UI}^*)\mathbf{H}_{BI}^*\mathbf{w}^*\mathbf{w}^T\mathbf{h}_{BU}^T \\ \mathbf{h}_{BU}^*\mathbf{w}^*\mathbf{w}^T\mathbf{H}_{BI}^T diag(\mathbf{h}_{UI}) & 0 \end{bmatrix},$$

$$\mathbf{G}_E=\frac{1}{\sigma_E^2}\begin{bmatrix} diag(\mathbf{h}_{EI}^*)\mathbf{H}_{BI}^*\mathbf{w}^*\mathbf{w}^T\mathbf{H}_{BI}^T diag(\mathbf{h}_{UI}) & diag(\mathbf{h}_{EI}^*)\mathbf{H}_{BI}^*\mathbf{w}^*\mathbf{w}^T\mathbf{h}_{BE}^T \\ \mathbf{h}_{BE}^*\mathbf{w}^*\mathbf{w}^T\mathbf{H}_{BI}^T diag(\mathbf{h}_{EI}) & 0 \end{bmatrix}.$$

Besides, the constrain (16b) can be expressed as $\mathbf{s}\mathbf{E}_n\mathbf{s}^H=1, \forall n$, and the $\mathbf{E}_n$ is a matrix of N-order, which the (n,n) element of it equals 1, the else are all 0.

By substituting (17) into the problem (16a), we rewrite the P2 into a more tractable form as

$$\max_{\mathbf{s}} \ \frac{\mathbf{s}^H\mathbf{G}_U\mathbf{s}+h_U+1}{\mathbf{s}^H\mathbf{G}_E\mathbf{s}+h_E+1}, \tag{18a}$$

$$\text{s.t.} \ \mathbf{s}\mathbf{E}_n\mathbf{s}^H=1, \forall n. \tag{18b}$$

Since (18b) is a non-convex quadratic equality constraint, and the objective function (18a) is fractional and non-concave with respect to $\mathbf{s}$. To tackle the non-convexity, the SDR method [15] is employed. Define $\mathbf{S}\triangleq\mathbf{s}\mathbf{s}^H$, problem (18) is reformulated as

$$\max_{\mathbf{S}} \ \frac{tr(\mathbf{G}_U\mathbf{S})+h_U+1}{tr(\mathbf{G}_E\mathbf{S})+h_E+1}, \tag{19a}$$

$$\text{s.t.} \ tr(\mathbf{E}_n\mathbf{S})=1, \forall n, \tag{19b}$$

$$rank(\mathbf{S})=1. \tag{19c}$$

Next, by applying the Charnes-Cooper transformation [16], and ignoring the rank-one constraint on $\mathbf{S}$, we define $\mu\triangleq 1/[tr(\mathbf{G}_E{}^*\mathbf{S})+h_E+1]$. Then, problem (19) can be transformed into the following form

$$\max_{\mu \geqslant 0, \mathbf{X}} \; tr(\mathbf{G}_U \mathbf{X}) + \mu(h_U + 1), \tag{20a}$$

$$\text{s.t. } tr(\mathbf{G}_E \mathbf{X}) + \mu(h_E + 1) = 1, \tag{20b}$$

$$tr(\mathbf{E}_n \mathbf{X}) = \mu, \forall n, \tag{20c}$$

where $\mathbf{X} = \mu^* \mathbf{S}$. Problem (20) is a standard semidefinite programming (SDP) problem [17], which can be solved by using the interior-point method [18,19].

3.3 Sub-problem 3: Optimizing the Position $\mathbf{C}_I$ of the AIRS with Given Q and w

According to (3)–(5), all channel gains are related to the distance between the transmitter and the receiver. The position of the AIRS determines the large-scale fading of $\mathbf{H}_{BI}$, $\mathbf{h}_{UI}$ and $\mathbf{h}_{EI}$. In this situation, we can detail the communication rate of the user and eavesdropper as

$$\begin{aligned} R_U &= \log_2(1 + \frac{|(\mathbf{h}_{UI}^T \mathbf{Q} \mathbf{H}_{BI} + \mathbf{h}_{BU})\mathbf{w}|^2}{\sigma_U^2}) \\ &= \log_2(1 + \frac{\rho |\mathbf{w}|^2}{\sigma_U^2} * |\frac{\mathbf{v}_{UI}^T \mathbf{Q} \mathbf{V}_{BI}}{\rho^{-\frac{1}{2}} d_{UI}^{\frac{\alpha}{2}} * d_{BI}^{\frac{\alpha}{2}}} + \frac{\mathbf{g}_{BU}}{d_{BU}^{\frac{\kappa}{2}}}|^2), \end{aligned} \tag{21a}$$

$$\begin{aligned} R_E &= \log_2(1 + \frac{|(\mathbf{h}_{EI}^T \mathbf{Q} \mathbf{H}_{BI} + \mathbf{h}_{BE})\mathbf{w}|^2}{\sigma_E^2}) \\ &= \log_2(1 + \frac{\rho |\mathbf{w}|^2}{\sigma_E^2} * |\frac{\mathbf{v}_{EI}^T \mathbf{Q} \mathbf{V}_{BI}}{\rho^{-\frac{1}{2}} d_{EI}^{\frac{\alpha}{2}} * d_{BI}^{\frac{\alpha}{2}}} + \frac{\mathbf{g}_{BE}}{d_{BE}^{\frac{\kappa}{2}}}|^2). \end{aligned} \tag{21b}$$

It is worth noting that d_{BI}, d_{UI}, d_{EI}, and $\mathbf{v}_{ZI}$ are relevant to the AIRS's trajectory. However, it is observed that $\mathbf{v}_{ZI}$ is complex and non-linear with respect to the AIRS's trajectory variables $\mathbf{C}_I$, which makes the trajectory design intractable. Then, subject to the AIRS mobility constraints in (1), we formulate the secrecy rate maximization problem as follows

$$\text{P3:} \max_{\mathbf{C}_I} \; R_{\text{sec}} = R_U - R_E \tag{22a}$$

$$s.t. \; \mathbf{C}_I \in \mathcal{X} \times \mathcal{Y}. \tag{22b}$$

Based on (21), we first introduce the slack variables inequality $m_U \leqslant d_{UI}^{-\frac{\alpha}{2}} * d_{BI}^{-\frac{\alpha}{2}}$ and $s_E \geqslant d_{EI}^{-\frac{\alpha}{2}} * d_{BI}^{-\frac{\alpha}{2}}$, respectively, and then introduce auxiliary variables f_U and k_E to transform the Eq. (21) into the following form

$$R_U \geqslant \log_2(1 + |\rho^{\frac{1}{2}} m_U \mathbf{v}_{UI}^T \mathbf{Q} \mathbf{V}_{BI} + d_{BU}^{-\frac{\kappa}{2}} \mathbf{g}_{BU}|^2) \geqslant \log_2(1 + \frac{\rho |\mathbf{w}|^2}{\sigma_U^2} * f_U), \tag{23}$$

$$R_E \leqslant \log_2(1 + |\rho^{\frac{1}{2}} s_E \mathbf{v}_{EI}^T \mathbf{Q} \mathbf{V}_{BI} + d_{BE}^{-\frac{\kappa}{2}} \mathbf{g}_{BE}|^2) \leqslant \log_2(1 + \frac{\rho |\mathbf{w}|^2}{\sigma_E^2} * k_E). \tag{24}$$

Then, for the worst case of secure communication, taking (23)–(24) into consideration, the P3 can be expressed as

$$\max_{\Omega} \ \log_2(1+\frac{\rho|\mathbf{w}|^2}{\sigma_U^2} * f_U) - \log_2(1+\frac{\rho|\mathbf{w}|^2}{\sigma_E^2} * k_E), \tag{25a}$$

$$s.t.\ \mathbf{C}_I \in \mathcal{X}\times\mathcal{Y}, \tag{25b}$$

$$d_{UI}^2 * d_{BI}^2 \leqslant m_U^{-\frac{4}{\alpha}}, \tag{25c}$$

$$d_{EI}^2 * d_{BI}^2 \geqslant s_E^{-\frac{4}{\alpha}}, \tag{25d}$$

$$\mathbf{J}_U * \mathbf{J}_{HU} * \mathbf{J}_U{}^T \geqslant f_U, \tag{25e}$$

$$\mathbf{J}_E * \mathbf{J}_{HE} * \mathbf{J}_E{}^T \leqslant k_E, \tag{25f}$$

$$\Omega = \{\mathbf{C}_I, f_U, k_E, m_U, s_E\}, \tag{25g}$$

where $\mathbf{J}_U = [\rho^{\frac{1}{2}} m_U, d_{BU}^{-\frac{\kappa}{2}}]$, $\mathbf{J}_{HU} = [\mathbf{v}_{UI}^T \mathbf{Q}\mathbf{V}_{BI}, \mathbf{g}_{BU}]^T * [\mathbf{v}_{UI}^T \mathbf{Q}\mathbf{V}_{BI}, \mathbf{g}_{BU}]$, $\mathbf{J}_E = [\rho^{\frac{1}{2}} s_E, d_{BE}^{-\frac{\kappa}{2}}]$, and $\mathbf{J}_{HE} = [\mathbf{v}_{EI}^T \mathbf{Q}\mathbf{V}_{BI}, \mathbf{g}_{BE}]^T * [\mathbf{v}_{EI}^T \mathbf{Q}\mathbf{V}_{BI}, \mathbf{g}_{BE}]$. We use the obtained AIRS position $\mathbf{C}_I$ from the last iteration to get an approximate $\mathbf{v}_{ZI}$ in this iteration [14]. In this way, we can make the problem (25) tractable with the slack variables m_U, s_E and the auxiliary variables f_U, k_E. The SCA technique can be applied to address the non-convex constraints (25c)–(25f) [9].

It is proved that d_{BI}^2 and d_{BI}^4 are convex functions of $\mathbf{C}_I$ [7]. Similarly, d_{EI}^2, d_{EI}^4, d_{UI}^2, d_{UI}^4 are all convex function of $\mathbf{C}_I$. However, (24d) and (24e) are still non-convex due to the terms $d_{UI}^2 * d_{BI}^2$ and $d_{EI}^2 * d_{BI}^2$. Next, we further process the upper bound function of $d_{UI}^2 * d_{BI}^2$ as

$$\begin{aligned} d_{UI}^2 d_{BI}^2 &= \frac{1}{2}[(d_{UI}^2 + d_{BI}^2)^2 - (d_{UI}^4 + d_{BI}^4)] \\ &\leqslant \frac{1}{2}[(d_{UI}^2 + d_{BI}^2)^2 - ((d_{UI}^{(l)})^4 + (d_{BI}^{(l)})^4)] \\ &- 2[(d_{BI}^{(l)})^2(\mathbf{C}_I^{(l)} - \mathbf{C}_B)^T + (d_{UI}^{(l)})^2(\mathbf{C}_I^{(l)} - \mathbf{C}_U)^T] * (\mathbf{C}_I - \mathbf{C}_I^{(l)}) \\ &\triangleq f(\mathbf{C}_I). \end{aligned} \tag{26}$$

Similarly, the lower bound of $d_{EI}^2 * d_{BI}^2$ can be written as

$$\begin{aligned} d_{EI}^2 d_{BI}^2 &= \frac{1}{2}[(d_{EI}^2 + d_{BI}^2)^2 - (d_{EI}^4 + d_{BI}^4)] \\ &\geqslant \frac{1}{2}[((d_{EI}^{(l)})^2 + (d_{BI}^{(l)})^2)^2 - (d_{BI}^4 + d_{EI}^4)] \\ &+ 2[(d_{BI}^{(l)})^2 + (d_{EI}^{(l)})^2](2\mathbf{C}_I^{(l)} - \mathbf{C}_B - \mathbf{C}_E)^T * (\mathbf{C}_I - \mathbf{C}_I^{(l)}) \\ &\triangleq g(\mathbf{C}_I), \end{aligned} \tag{27}$$

where $d_{BI}^{(l)}$, $d_{UI}^{(l)}$, $d_{EI}^{(l)}$, and $\mathbf{C}_I^{(l)}$ are the variables obtainted from last iteration. In the right side of (25c) and (25d), $m_U^{-\frac{4}{\alpha}}$ and $s_E^{-\frac{4}{\alpha}}$ are convex functions. However, (25d) can not satisfy inequality optimization condition. The first-order Taylor

expansion is applied to make the constraint (25d) feasible, which is expressed as

$$m_U^{-\frac{4}{\alpha}} \geqslant (m_U^{(l)})^{-\frac{4}{\alpha}} - \frac{4}{\alpha}(m_U^{(l)})^{-\frac{4}{\alpha}-1}(m_U - m_U^{(l)}), \tag{28}$$

where $m_U^{(l)} = d_{BI}^{(l)-\frac{\alpha}{2}} d_{UI}^{(l)-\frac{\alpha}{2}}$. Then, the left side of expression (25e) is the standard quadratic function. We try to use the first-order Taylor expansion, which approximatively address the non-convex constrain (25e) as follow [14]

$$\mathbf{J}_U * \mathbf{J}_{HU} * \mathbf{J}_U^T \geqslant 2\Re(\mathbf{J}_{U0} * \mathbf{J}_{HU} * \mathbf{J}_{U0}^T) - \mathbf{J}_{U0} * \mathbf{J}_{HU} * \mathbf{J}_U^T \geqslant f_U, \tag{29}$$

where $\mathbf{J}_{U0} = [\rho^{\frac{1}{2}} m_U^{(l)}, d_{BU}^{-\frac{\kappa}{2}}]$. According to the expression (25a), it is non-convex with the variable k_E, which make the object function untracked for maximization. Similarly, the first-order Taylor expansion could approximate the R_E as

$$R_E \leqslant \log_2(1 + \frac{\rho|\mathbf{w}|^2}{\sigma_E^2} * k_E) \leqslant \log_2(1 + \frac{\rho|\mathbf{w}|^2}{\sigma_E^2} * k_E^{(l)}) + \frac{\frac{\rho|\mathbf{w}|^2}{\sigma_E^2}(k_E - k_E^{(l)})}{\ln 2(1 + \frac{\rho|\mathbf{w}|^2}{\sigma_E^2} * k_E^{(l)})} \tag{30}$$

where $k_E^{(l)} = |\rho^{\frac{1}{2}} s_E^{(l)} \mathbf{v}_{EI}^T \mathbf{Q} \mathbf{V}_{BI} + d_{BE}^{-\frac{\kappa}{2}} \mathbf{g}_{BE}|^2$ and $s_E^{(l)} = d_{EI}^{(l)-\frac{\alpha}{2}} d_{BI}^{(l)-\frac{\alpha}{2}}$. According to (26)–(30), the convex optimization problem can be expressed as

$$\text{P4:} \max_{\Omega} \ \log_2(1 + \frac{\rho|\mathbf{w}|^2}{\sigma_U^2} * f_U) - \frac{\frac{\rho|\mathbf{w}|^2}{\sigma_E^2} * k_E}{\ln 2(1 + \frac{\rho|\mathbf{w}|^2}{\sigma_E^2} * k_E^{(l)})}, \tag{31a}$$

$$s.t. \ \mathbf{C}_I \in \mathcal{X} \times \mathcal{Y}, \tag{31b}$$

$$f(\mathbf{C}_I) \leqslant (m_U^{(l)})^{-\frac{4}{\alpha}} - \frac{4}{\alpha}(m_U^{(l)})^{-\frac{4}{\alpha}-1}(m_U - m_U^{(l)}), \tag{31c}$$

$$s_E^{-\frac{4}{\alpha}} - g(\mathbf{C}_I) \leqslant 0, \tag{31d}$$

$$2\Re(\mathbf{J}_{U0} * \mathbf{J}_{HU} * \mathbf{J}_{U0}^T) - \mathbf{J}_{U0} * \mathbf{J}_{HU} * \mathbf{J}_U^T \geqslant f_U, \tag{31e}$$

$$\mathbf{J}_E * \mathbf{J}_{HE} * \mathbf{J}_E^T - k_E \leqslant 0, \tag{31f}$$

$$\Omega = \{\mathbf{C}_I, f_U, k_E, m_U, s_E\}. \tag{31g}$$

By incorporating a quasi-convex objective and all convex constraints, P4 is the approximate convex transformation of the problem (25), which can be solved by convex optimization software such as CVX. Then, the original problem P3 can be tackled by solving a series of P4 iteratively.

3.4 Overall Algorithm

With the solutions to the three sub-problems, the overall algorithm for solving P0 is summarized in Algorithm 1, where $\mathbf{1}_M$ denotes an M-dimension vector whose elements are all 1, ε is used for the accuracy of iterations, and $k_{\max}$ denote the maximum number of iterations.

Algorithm 1. Proposed AO Algorithm

1: Initialization: set $k = 0$; the origin $\mathbf{C}_I^{(0)}$ and phase shift $\mathbf{q}^{(0)}$ of AIRS randomly; $\mathbf{w}^{(0)} = \mathbf{1}_M$;
2: Get the CSI of system channels and $R_{\text{sec}}^{(0)} = f(\mathbf{C}_I^{(0)}, \mathbf{q}^{(0)}, \mathbf{w}^{(0)})$;
3: **repeat**
4: $k \leftarrow k + 1$;
5: Update $\mathbf{w}^{(k)}$ based on (15);
6: Update $\mathbf{q}^{(k)}$ based on the result of problem (20);
7: Update $\mathbf{C}_I^{(k)}$ based on the result of problem (31);
8: Update the CSI of system channels and $R_{\text{sec}}^{(k)} = f(\mathbf{C}_I^{(k)}, \mathbf{q}^{(k)}, \mathbf{w}^{(k)})$;
9: **until** $|R_{\text{sec}}^{(k)} - R_{\text{sec}}^{(k-1)}| \leqslant \varepsilon$ or $k \geqslant k_{\max}$.
Output: The optimal position of AIRS and the convergency value of R_{sec}

4 Simulation Results

In this section, we analyze the performance of the proposed AO algorithm through numerical results. The following benchmark algorithms are used for comparison:

- Only optimizing the AIRS's trajectory, neglecting the BS transmit beamforming and the phase shift of AIRS (denoted as only trajectory optimization)
- Fixed the position of AIRS at the origin point, optimizing the transmit beamforming and the phase shift of AIRS jointly (denoted as fixed AIRS)

We consider a situation that the BS, the user, and the eavesdropper are located at (100, 0), (120, 90), (60, 60), respectively (distance in maters). The AIRS is flying in the horizon plane with an altitude of $z_I = 100\,\text{m}$, and the traveling range of AIRS is a square within $\mathcal{X} \sim [50\,\text{m}, 130\,\text{m}]$, $\mathcal{Y} \sim [0\,\text{m}, 100\,\text{m}]$. The AIRS elements are arranged in a square and the number is $N \leq 100$, and the ratios of the element separation and the antenna separation with wavelength are set as $\Delta d/\lambda = 0.5$ and $\Delta a/\lambda = 0.5$, respectively. The background noise power is -150 dBW, and the BS's maximum transmit power is $P_{\text{BS}} = 1\,\text{W}$. For path loss relating parameters, we set $\rho = -30$ dB, the ground channels experience a path loss exponent of $\kappa = 3.5$, while the air-ground channels $\alpha = 2.4$. Besides, the convergence threshold is setting as $\varepsilon = 10^{-3}$ and $k_{\max} = 50$.

In Fig. 1, we present the progress of the AIRS to search the optimal position from different origins and the convergence behavior of the algorithm in subproblem 3. The number of the reflection elements is set as $N = 64$, and the ground units of the BS, the user and the eavesdropper stay at the permanent position. During the SCA algorithm iteration, the trajectory of AIRS is updated with the new optimized coordinates. Fig. 1(a) presents the AIRS's trajectory of the different situations. They converg to the same optimal position (110, 45), even the worst situation (70, 10). Besides, different from the UAV transmitter or relay system in which the UAV fly to the user side to assist communication security [6], the AIRS flies directly to the optimal position in the situation of origin (120, 80). In Fig. 1(b),

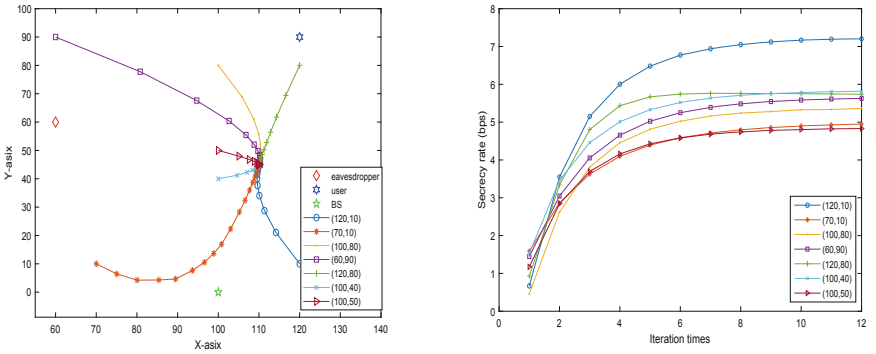

(a) AIRS's trajectory of different origins (b) The convergence behavior

Fig. 1. AIRS's trajectory and the algorithm convergence behavior w.r.t different origins

we show the secrecy rate convergence behavior of the proposed algorithm in subproblem 3 under different AIRS trajectories. It is observed that our proposed algorithm can quickly converge after around 10 iterations. That the converged secrecy rate is mainly distributed around 5 bps due to the CSCG random component $\mathbf{g}_{BU}$ and $\mathbf{g}_{BE}$ of the directed channel gains from the BS to the user and eavesdropper, the two gains are important parts of receiving signals.

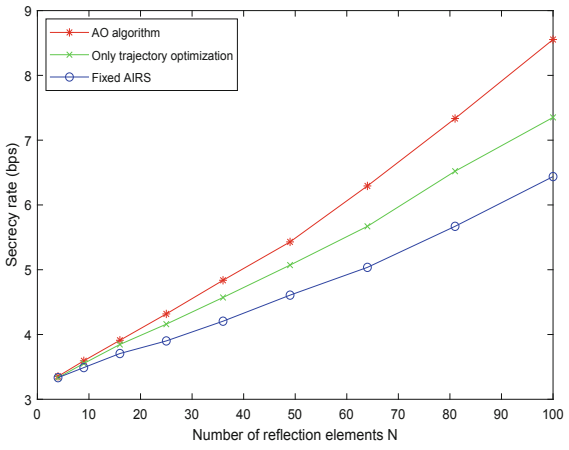

Fig. 2. Secrecy rate behavior versus the number of reflecting elements N

In Fig. 2, we compare the secrecy rate performance of the proposed AO algorithm with the benchmark algorithms in the case of reflection elements, and the secrecy rate of each N is the average of the different situations in Fig. 1(b). From Fig. 2, we can see that the secrecy rate all increases as the number of

reflection elements grows, and that of AO algorithm is higher than the other two. In addition, the AIRS' trajectory optimization is more efficient than the fixed AIRS, since the reflection signal strength of the user is greater than that of the eavesdropper when the AIRS moves to the optimal position. As the number of reflection elements increases, the reflection signals are superposed at the user side, which makes the gap larger.

5 Conclusion

In this paper, we have investigated the UAV equipped with an IRS to assist the ground secure communication. The transmit beamforming vector, the reflection phase shift and trajectory of the AIRS are jointly optimized to maximize the secure transmission rate. Utilizing the AO framework, we have applied the SDP and SCA methods to solve the original problem iteratively. Numerical results show that the proposed algorithm converges fastly and is effective for improving the secrecy rate. Also, it reveal that the trajectory optimization is higher-efficiency to enhance the secrecy rate than the fixed AIRS, and jointly optimized the transmit beamforming vector, the reflection phase shift and trajectory of AIRS can combine the different roles of UAV and IRS to enhance secure communication.

References

1. Wu, Q., Zhang, S., Zheng, B., You, C., Zhang, R.: Intelligent reflecting surface-aided wireless communications: a tutorial. IEEE Trans. Commun. **69**(5), 3313–3351 (2021)
2. Sun, W., Song, Q., Guo, L., Zhao, J.: Secrecy rate maximization for intelligent reflecting surface aided SWIPT systems. In: 2020 IEEE/CIC International Conference on Communications in China (ICCC), pp. 1276–1281 (2020). https://doi.org/10.1109/ICCC49849.2020.9238963
3. Cui, M., Zhang, G., Zhang, R.: Secure wireless communication via intelligent reflecting surface. IEEE Wirel. Commun. Lett. **8**(5), 1410–1414 (2019)
4. Hong, S., Pan, C., Zhou, G., Ren, H., Wang, K.: Outage constrained robust transmission design for IRS-aided secure communications with direct communication links (2020). https://arxiv.org/abs/2011.09822
5. Zhang, G., Wu, Q., Cui, M., Zhang, R.: Securing UAV communications via joint trajectory and power control. IEEE Trans. Wirel. Commun. **18**(2), 1376–1389 (2019)
6. Shen, L., Wang, N., Ji, X., Mu, X., Cai, L.: Iterative trajectory optimization for physical-layer secure buffer-aided UAV mobile relaying. Sensors **19**(15), 3442 (2019)
7. Long, H., et al.: Reflections in the sky: joint trajectory and passive beamforming design for secure UAV networks with reconfigurable intelligent surface (2020). https://arxiv.org/abs/2005.10559
8. Zhang, Q., Saad, W., Bennis, M.: Reflections in the sky: millimeter wave communication with UAV-carried intelligent reflectors. In: 2019 IEEE Global Communications Conference (GLOBECOM), pp. 1–6 (2019). https://doi.org/10.1109/GLOBECOM38437.2019.9013626

9. Tang, X., Wang, D., Zhang, R., Chu, Z., Han, Z.: Jamming mitigation via aerial reconfigurable intelligent surface: Passive beamforming and deployment optimization. IEEE Trans. Veh. Technol. **70**(6), 6232–6237 (2021)
10. You, C., Kang, Z., Zeng, Y., Zhang, R.: Enabling smart reflection in integrated air-ground wireless network: IRS meets UAV (2021). https://arxiv.org/abs/2103.07151
11. Cai, Y., Wei, Z., Hu, S., Ng, D.W.K., Yuan, J.: Resource allocation for power-efficient IRS-assisted UAV communications. In: 2020 IEEE International Conference on Communications Workshops (ICC Workshops), pp. 1–7 (2020). https://doi.org/10.1109/ICCWorkshops49005.2020.9145224
12. Zheng, B., You, C., Zhang, R.: Intelligent reflecting surface assisted multi-user OFDMA: channel estimation and training design. IEEE Trans. Wirel. Commun. **19**(12), 8315–8329 (2020)
13. He, Z.Q., Yuan, X.: Cascaded channel estimation for large intelligent metasurface assisted massive MIMO. IEEE Wirel. Commun. Lett. **9**(2), 210–214 (2020)
14. Li, S., Duo, B., Di Renzo, M., Tao, M., Yuan, X.: Robust secure UAV communications with the aid of reconfigurable intelligent surfaces. IEEE Trans. Wirel. Commun. 1 (2021). https://doi.org/10.1109/TWC.2021.3073746
15. Chu, Z., Hao, W., Xiao, P., Shi, J.: Intelligent reflecting surface aided multi-antenna secure transmission. IEEE Wirel. Commun. Lett. **9**(1), 108–112 (2020)
16. Liu, L., Zhang, R., Chua, K.C.: Secrecy wireless information and power transfer with miso beamforming. IEEE Trans. Signal Process. **62**(7), 1850–1863 (2014)
17. Boyd, S., Vandenberghe, L.: Convex Optimization. Cambridge University Press, Cambridge (2004)
18. Pólik, I., Terlaky, T.: Interior point methods for nonlinear optimization. In: Di Pillo, G., Schoen, F. (eds.) Nonlinear Optimization. Lecture Notes in Mathematics, vol. 1989, pp. 215–276. Springer, Heidelberg (2010). https://doi.org/10.1007/978-3-642-11339-0_4
19. So, A.M.C., Zhang, J., Ye, Y.: On approximating complex quadratic optimization problems via semidefinite programming relaxations. Math. Program. **1**(10), 93–110 (2007)